UV-Induced Desorption-Retrapping Cycle of Electrochemically Adsorbed CO on Pt(111) Surface

N. Ohta, Q.-K. Yu, and S. Nakabayashi*

Department of Chemistry, Faculty of Science, Saitama University, 255 Shimo-ohkubo, Urawa, Saitama 338-8570, Japan

Received: August 17, 2000; In Final Form: December 15, 2000

UV irradiation (266 nm) from a nanosecond and/or a femtosecond laser-induced reconstruction of CO adsorbed layer on Pt(111) electrode. The current peak shape in the cyclic voltammogram (CV) for the electrochemical oxidation of the adsorbed CO was varied by the irradiation, which did not leave any change in the CV response on the adsorption free Pt(111) surface. Although the current peak shape in the CV was changed, the total charge for the CO oxidation remained constant. The green light irradiation (532 nm) from the lasers did not induce any change in the CV. These findings suggested that the UV induced CO desorption and re-trapping cycles were sustained on the electrode surface, which passed through electronic excited states at the surface.

1. Introduction

An electronic excitation of the adsorption bond on the well-defined solid surface has attracted the great interest in past decades.[1−4] The optical control of the interaction between the solid surface and the adsorbed species has a potential to open the door to a new technology such as precise patterning of the adsorption layer. It is also very important from the fundamental point of view in physical chemistry.

The most cultivated systems in the surface photochemistry is the CO or NO molecules adsorbed on the Pt(111) surface.[5−7] The detailed information has been accumulated by RAIR, REMPI and ESD.[8] In this article, we would like to extend the study of the system to electrochemical interface. For the electrochemical study in an aqueous electrolyte, however, the NO/Pt(111) is rather complicated because NO is protonated in the solution. Therefore, we chose the CO/Pt(111) in this experiment.

2. Experimental Section

The Pt(111) single crystal used in this experiment was made by the Clavilier method.[9−11] The Pt ball was cut parallel to the (111) facet using the laser alignment technique. The quality of the surface was checked by measuring the CV response in a 0.5 M sulfuric acid aqueous electrolyte. The polishing and annealing cycles were repeated until the CV identical with the one of the previous reports[12] was obtained. The current peak shape of the CV especially in the hydrogen UPD region is structure-sensitive and can be considered as the fingerprint of the surface quality. We measured the CV before and after every laser desorption experiment to avoid an unexpected artifact such as the contamination of the surface, etc. In this way, the orthodox current peak shape obtained confirmed that the clean and well-defined surface was established.

The electrochemical cell and the optical configurations for the laser excitation are shown schematically in Figure 1. The adsorption of CO was followed by the procedure; CO was bubbled into the electrolyte for 3 min. After termination of the CO bubbling, N_2 or Ar was bubbled in order to purge the dissolved CO from the electrolyte. For the CO adsorption process, the electrode potential was kept −0.25 V vs SCE. The UV irradiation and the electrochemical measurements were conducted under N_2 or Ar gas flow over the surface of the electrolyte. Only Pt(111) surface was contacted with the electrolyte by the meniscus contact technique.

Two regimes of laser desorption were studied; nano-second and femtosecond. For nanosecond irradiation, the fourth harmonic of Nd:YAG laser was used (Coherent Infinity 40−100, fwmh 3.5 ns, 15−50 mJ pulse^{-1} at 1064 nm, repetition rate 20 Hz). The fourth harmonics at 266 nm was obtained through a successive optical doubling of the laser output by the nonlinear crystals. The other harmonics were filtered by prisms. For femtosecond irradiation, the output from the Clark-MXR CPA-2000 (an Er doped fiber laser coupled with a regenerative amplifier, fwhm 150 fsec) was optically tripled by the combination of nonlinear crystals. The repetition rate was 1 kHz and the pulse energy was 0.9 mJ pulse^{-1} at 800 nm. For both regimes, we used unfocused beam at the normal incidence. The power of the laser pulse was measured by a laser power meter (Genetic TPM-330). The electrochemical measurements were conducted by using a potentiostat (model 273 EG&G PARC) and a X−Y recorder (Yokogawa 3036). The scheme for the potential scanning was shown at the inset in Figure 1.

3. Results

3.1. Nanosecond Irradiation under Resonant Condition.

The effect of the nano-second laser irradiation to the electrochemical oxidation of CO/Pt(111) in 0.5 M sulfuric acid aqueous electrolyte is shown in Figure 2. Without laser irradiation, the sharp single anodic peak was observed in Figure 2 (a) around 0.4 to 0.6 V. It arises due to the electrochemical oxidation of the surface adsorbed CO. The overall electrochemical reaction can be described as

$$CO_{ad} + H_2O \rightarrow CO_2 + 2H^+ + 2e^-$$

where CO_{ad} represents the surface adsorbed CO. After the oxidation of CO_{ad}, the surface became CO-free Pt(111). Then, under cathodic potential scanning, the three typical cathodic peaks were successively obtained at 0.4, 0.2, and 0 V. One of

10.1021/jp0029820 CCC: $20.00
Published on Web 03/30/2001

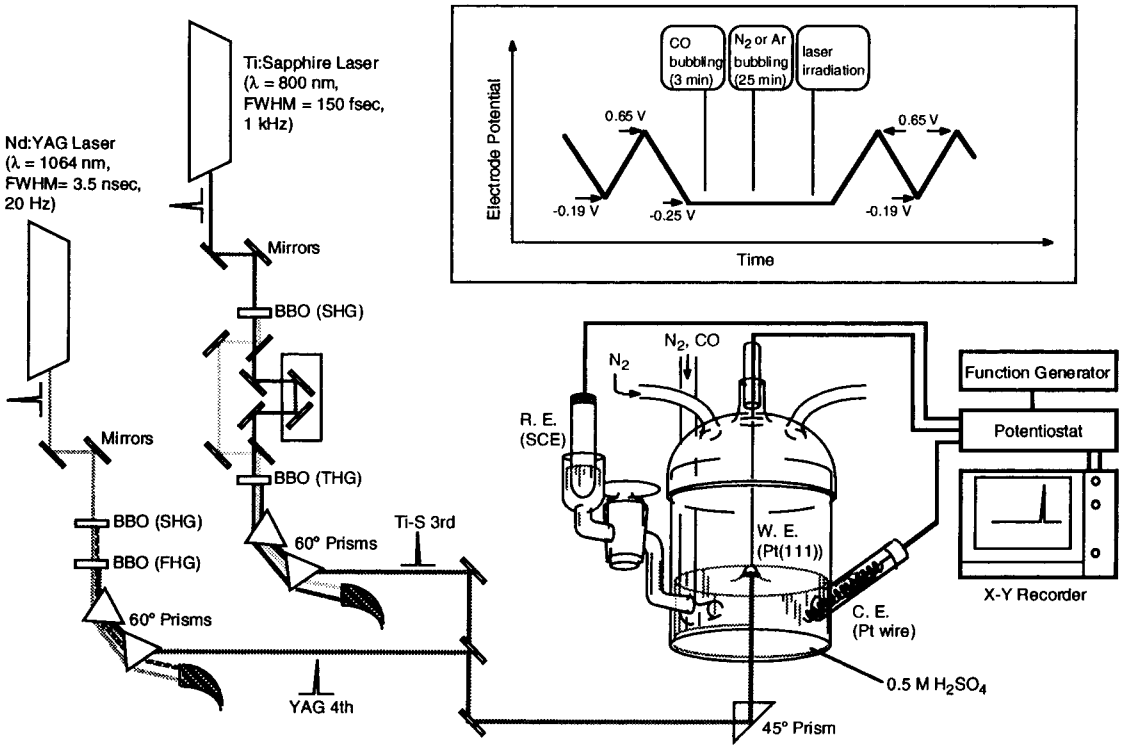

Figure 1. Schematic representation of experimental setup. The potential scheme was shown in the upper inset.

them (0 V) was accompanied by the plateau. In the following anodic potential scan, the almost symmetric anodic CV features were obtained. The current peak shape after the oxidation of CO_{ad} was expanded and shown in Figure 2a′. The current peaks, which were obtained during potential scan from the cathodic toward the anodic direction, can be identified with the UPD of the hydrogen atom, the adsorption of the bisulfate ion and the OH adsorption on the electrode surface.[9,12] Figure 2a′ shows that the platinum surface appeared after the oxidation of CO_{ad} is (111) oriented, well-ordered, and noncontaminated.

After the successive laser irradiation for 5 min with 75 mW cm^{-2}, the CV changed to Figure 2b. The total energy of the incident photons was 22.5 J cm^{-2} for Figure 2b. The height of the CO oxidation peak decreased, and the width of the peak was enlarged. Although the current peak shape for the electrochemical oxidation of CO changed, the peaks attributed to hydrogen, bisulfate ion and OH adsorption on Pt(111) were not influenced by the laser irradiation as shown in Figure 2b′. This shows the laser irradiation induced no change in the uppermost platinum layer on the electrode. After the successive laser irradiation for 5 min with 150 mW cm^{-2}, where the formal input energy was 45 J cm^{-2}, the shape of the CV changed to Figure 2c and c′. As the increase of the 266 nm energy input, the height of the CO oxidation peak decreased and the width was enlarged without any change in the uppermost atomic configuration on Pt(111) surface. Furthermore, the total charge for the CO oxidation peak was constant, which shows the total amount of the CO molecules adsorbed on the surface was not changed by the laser irradiation.

The total charge for the CO_{ad} oxidation was $\cong$550 μC cm^{-2}. According to the method proposed by Markivic et al.,[12] the charge for electrooxidation of CO_{ad} (Q_{CO}) estimated from aforementioned total charge is $\cong$410 μC cm^{-2}. The number of surface sites on Pt(111) is 1.50×10^{15} cm^{-2}. Thus, the coverage of CO_{ad} 1.28×10^{15} molecules cm^{-2}, calculated from Q_{CO}, corresponds to a coverage of $\cong$0.85 ML in assuming that the adsorption structure of CO is p(2 × 2)-3CO.

3.2. Nanosecond Irradiation under Off-Resonant Condition. To confirm a resonant character of the desorption process, we performed an identical experiment but with the use of a visible (the second harmonic of Nd:YAG) laser at 532 nm. The results are shown in Figure 3, where the input optical energy increased from a to c. The formal input energy was 0, 22.5, and 45 J cm^{-2} for Figure 3a, b, and c, respectively. Up to 45 J cm^{-2}, the shape of the electrochemical CO oxidation peak was not changed. And also, the laser irradiation did not induce any change in the CV after the oxidation of CO_{ad} as shown in Figure 3a′−c′.

3.3. Comparison between the Nanosecond Irradiations. The change in the shape of the CO oxidation peak was plotted for several independent experiments as shown in Figures 4 and 5 for 266 and 532 nm irradiation, respectively. Under the 266 nm irradiation, the total charge for the CO oxidation was constant as shown in Figure 4a. However, the maximum current decreased and the width of the peak enlarged as shown in Figure 4b and c), respectively. In the case of the 532 nm irradiation, these three parameters; the total charge, the maximum current and the width of the peak were almost constant as shown in Figure 5.

3.4. Femtosecond Irradiation. The change in the CO electrooxidation shape in the voltammogram was demonstrated in Figure 6 under the irradiation of the third harmonics (266 nm) of the Ti:sapphire laser. The width of the laser pulse measured by the autocorrelation technique was 150 femtosecond. The total charge for the CO electro-oxidation was constant as shown in Figure 6a. However, the maximum current decreased and the width of the peak increased as shown in Figure 6b,c, respectively. These results obtained in Figure 6 was almost identical with the ones in Figure 4, although the duration of the laser was different about 10^4.

3.5. Stability of the Outermost Layer of Pt(111). An introduction of the defect sites by the laser irradiation has been reported on the perfectly smooth Pt(111) surface in the UHV conditions even though the incident power density was far below

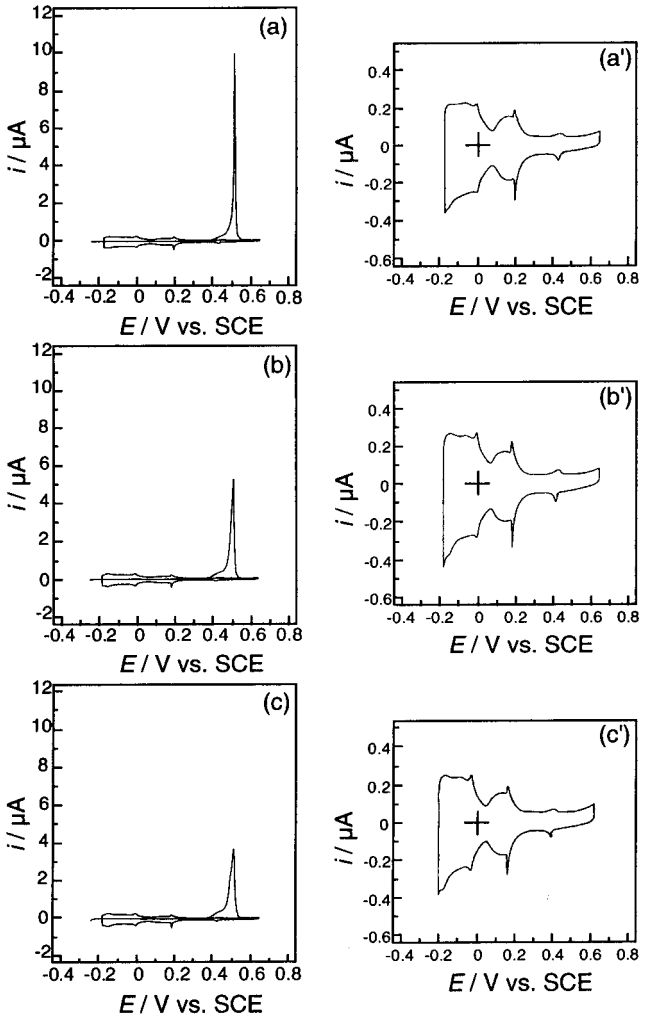

Figure 2. CO stripping voltammograms on CO/Pt(111) and the following base voltammograms on Pt(111) contacted with 0.5 M H_2SO_4 aqueous electrolyte. The potential sweep rate and the electrode surface area were 10 mV s^{-1} and 0.03 cm^2, respectively. No laser pulse irradiated at (a), but the successive laser pulse (λ = 266 nm, fwhm; 3.5 ns, repetition rate; 20 Hz) irradiated for 5 min with 3.75 mJ cm^{-2} $pulse^{-1}$ and 7.5 mJ cm^{-2} $pulse^{-1}$ at b and c, respectively. Figures a′−c′ show magnification of CV features obtained after CO electrooxidation.

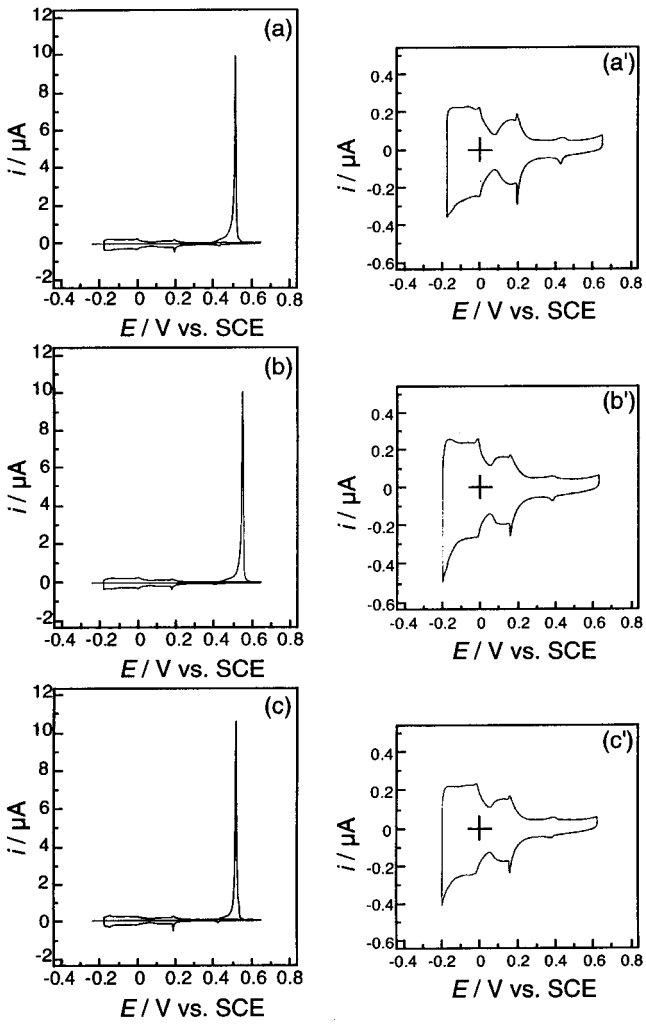

Figure 3. CO stripping voltammograms on CO/Pt(111) and the following base voltammograms on Pt(111) contacted with 0.5 M H_2SO_4 aqueous electrolyte. The potential sweep rate and the electrode surface area were 10 mV s^{-1} and 0.03 cm^2, respectively. No laser pulse irradiated at (a), but the successive laser pulse (λ = 532 nm, fwhm; 3.5 ns, repetition rate; 20 Hz, pulse energy; 7.5 mJ cm^{-2} $pulse^{-1}$) irradiated for 2.5 and 5 min at b and c, respectively. Figures a′−c′ show magnification of CV features obtained after CO electrooxidation.

the threshold of the surface melting.[13] The photoinduced defects can be evaluated by the change in the thermal desorption spectrum of CO in UHV conditions.[13] However, under the electrochemical conditions, the most sensitive spectrum for the atomic modification on Pt(111) surface is the CV in the aqueous sulfuric acid electrolyte. The typical CVs were shown in Figure 7a−d, which were obtained after the successive irradiation of 266 nm pulse (fwhm 3.5 ns) without any adsorption molecule on the surface. Formal input energy into the surface was 0, 22.5, 45, and 90 J cm^{-2} for Figure 7a−d, respectively. Up to 45 J cm^{-2}, the shape of the voltammogram did not change as shown in Figure 7a−c, but after the irradiation of 90 J cm^{-2}, it changed as shown in Figure 7d. Then, it is very sure that the atomic configuration on the outermost layer of Pt(111) is well ordered below the fluence of 45 J cm^{-2}.

To check the stability of the CO adsorption layer, the CVs shown in Figure 8 were obtained. The CO electrooxidation peak as shown in Figure 8a was obtained after following pretreatments: (1) CO adsorption at −0.25 V under 3 min CO bubbling and (2) Ar bubbling for 60 min under dark condition while the potential was kept constant at −0.25 V. This current peak shape is consistent with Figure 2a, and any serious change cannot be observed between the two. After this electro-oxidation of CO, Figure 8b was obtained.

On the basis of these stability data shown in Figures 7 and 8, the change in the electrochemical CO oxidation peak as shown in Figures 2, 4, and 6 must be induced by the change in the geometry of the CO adsorption layer, which is caused by the laser irradiation.

4. Discussion

4.1. Photodesorption Mechanism. The mechanism of the CO desorption induced by ultraviolet laser irradiation was well studied in UHV conditions.[5] As for the irradiation of a nanosecond laser pulse, the photodesorption proceeded as a single photon process for 193 nm photon. The energy distribution into the desorbed CO molecule could be examined by the resonance-enhanced multiphoton ionization (REMPI) spectrum; the translational temperatures ($T_t = \langle E_t \rangle / 2k_B$) were 2060 ± 250 and 2140 ± 170 K for v = 0 and v = 1, respectively. The average temperature of the rotational, vibrational and translational

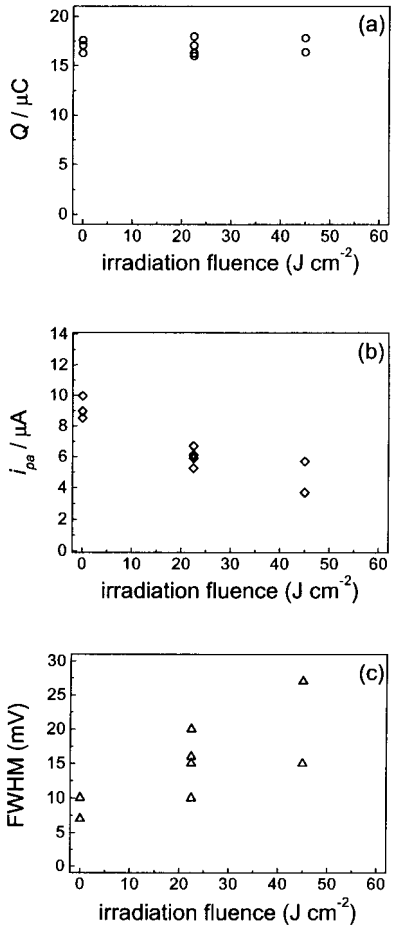

Figure 4. Dependence of the total charge for the CO oxidation (a), the maximum current i_{pa} (b), and the width of the peak (c) on the 266 nm (fwhm; 3.5 ns) irradiation fluence.

motions were 130, 3700, and 2000 K, which were considerably higher than the sample temperature. Most interestingly, only the CO adsorbed at the on-top site on Pt(111) was desorbed by the UV irradiation, but the CO adsorbed at the bridge and/or the 3-fold coordinated sites were not desorbed.

Under the UHV conditions, the photocreated hot CO molecules can escape from the surface without any loss of energy because the energy migration by collision was not proceeded. However, in the electrochemical interface, if the hot molecule is created by the photodesorption, it must be cooling by the energy dissipation into the viscous motions of the electrolyte. Then, the photodesorbed molecule cannot escape from the surface by this cage effect of the liquid. Then, it is certainly retrapped at the surface.

To examine the mechanism for this photodesorption, the reaction yield was measured as a function of the polarization direction of the incident laser beam, where the incident angle of the beam was restricted to be 10° by the geometry of the electrochemical cell. The reaction yield was roughly estimated by the decrease in the height of the anodic peak. Under the irradiation of the p-polarized light, the yield was enhanced 20 % compared with the one obtained under the s-polarized excitation. If the optical transition dipole of the CO/Pt(111) is normal to the surface, this adsorption bond cannot be electrically excited by the s-polarized irradiation.[5,8,16] However, the case of the photodesorption under the UHV conditions, the s-polarized irradiation was also able to desorb the surface trapped CO at Pt(111).[5] Thus, these ambiguous situation was obtained in the electrochemical case as well as in the UHV case.

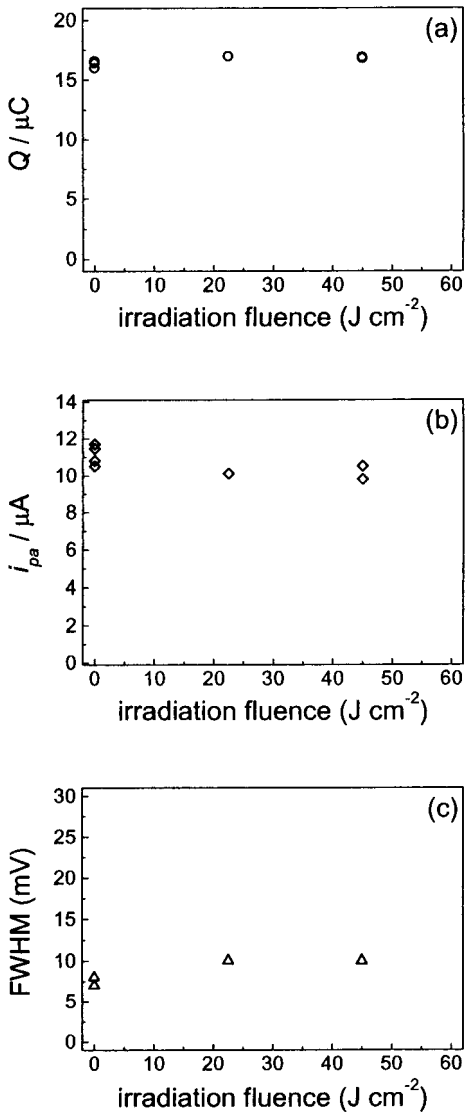

Figure 5. Dependence of the total charge for the CO oxidation (a), the maximum current i_{pa} (b), and the width of the peak (c) on the 532 nm (fwhm; 3.5 ns) irradiation fluence.

Tentatively, because the 532 nm excitation did not induce any change in both cases, we expect that the electrochemical photodesorption occurring by the nano-second irradiation of 266 nm light was proceeding through the electronic excitation of the adsorption bond of the atop CO on the Pt(111) electrode, which is the same mechanism proposed for the photodesorption in the UHV conditions.[5]

The alternative mechanism for the photodesorption, which proceeds without the direct optical excitation of the adsorption bond is the scheme named DIMET; desorption induced by multiple electronic transitions.[17−19] The desorption channel through DIMET is activated under the femtosecond laser irradiation. An optical absorption occurring in the metal creates the large amount of hot electrons because of the extremely high photon density within the duration of the laser pulse. Some of the hot electron can be trapped by the adsorbed molecule on the metal surface if the acceptor energy state locates energetically lower than the one of the hot electron. Thus, the adsorbed molecule is charged negatively in a very short time while the electron is localized at the molecule. After this, the electron on the molecule is inversely transferred into the top of the Fermi level in the metal. The large population of the hot electron enables to circulate this charge relaxation through the adsorption

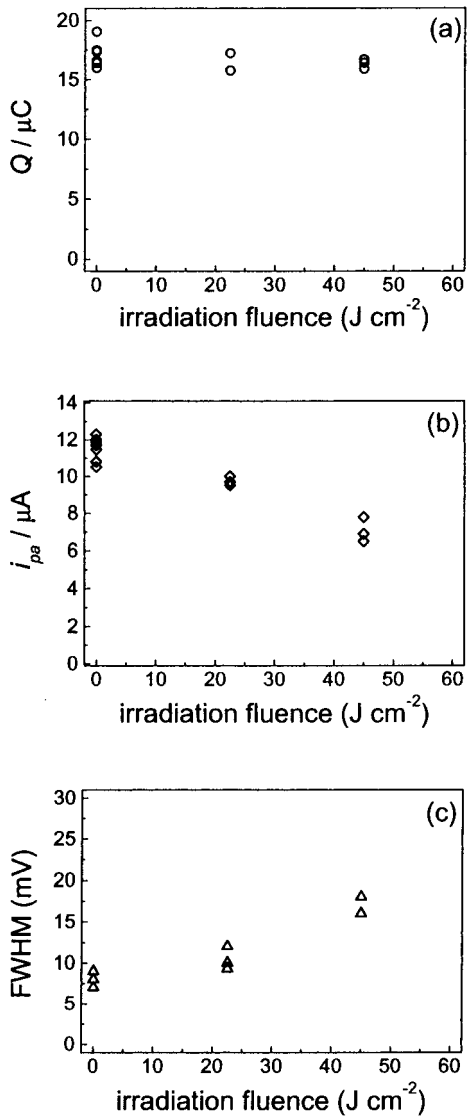

Figure 6. Dependence of the total charge for the CO oxidation (a), the maximum current i_{pa} (b), and the width of the peak (c) on the 266 nm (fwhm; 150 fs) irradiation fluence.

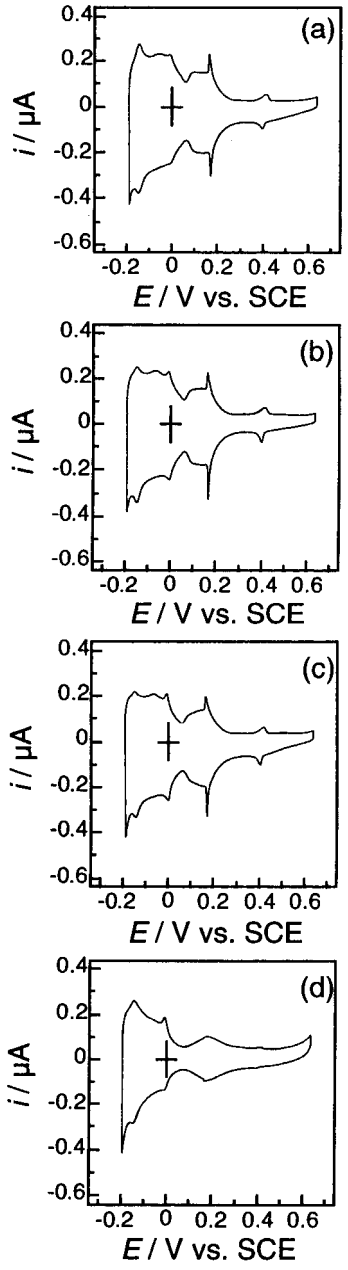

Figure 7. The base voltammograms on Pt(111) contacted with 0.5 M H_2SO_4 aqueous electrolyte. The fluence of the 266 nm irradiation (fwhm; 3.5 ns) was 0, 22.5, 45, 90 J cm^{-2} for a−d, respectively.

molecule in many times. The equilibrium bond length between the surface and the adsorbed molecule is shortened, while the adsorbed molecule is negatively charged because of the Coulombic attractive interaction between the negatively charged molecule and the image charge in the metal. Then, the multiple cycles of the electron trapping and releasing on the adsorbed molecule gradually activate the vibration of the adsorption bond and finally some of the molecules desorb from the surface.

The cross section for the photodesorption was reported to be a few orders of magnitude larger under the femtosecond irradiation than the one obtained under the nano-second excitation in the UHV case.[17−19] The recent optical up-conversion experiment using the sum frequency generation technique has revealed that the lifetime of the vibrational excited state of the adsorbed molecule was almost the same whether the surface was contacted with UHV or the electrolyte solution.[20,21] This is because the main energy dissipation channel for quenching the vibrational excited state is due to the energy flow to the free electrons in the metal. Then, the photodesorption cross section by the femtosecond irradiation is supposed to be much larger than the one by the nanosecond irradiation even in the electrochemical conditions. Therefore, the fact that the deformation of the electro-oxidation of CO was almost identical between the nano- and femtosecond excitation implies that the rate-determining step for the deformation was not the desorption process but the re-trapping process.

4.2. Photodesorption and Retrapping Cycle. The deformed shape of the voltammogram for the electrochemical CO oxidation can be deconvoluted into three components; the most anodic sharpest peak, the relatively broad peak, and the broadest component appeared in the most cathodic region. These three components were previously reported under nonirradiative experiment.[12] As shown in Figure 9, the deformed shape for the electrochemical oxidation of the surface adsorbed CO after the successive irradiation was able to be deconvoluted by using these three basis sets. Qualitatively, the photoirradiation induced the decrease in the most anodic component and the increase in the middle component. These increases and decreases of the peaks compensated each other; the total amount of the oxidation charge was kept constant.

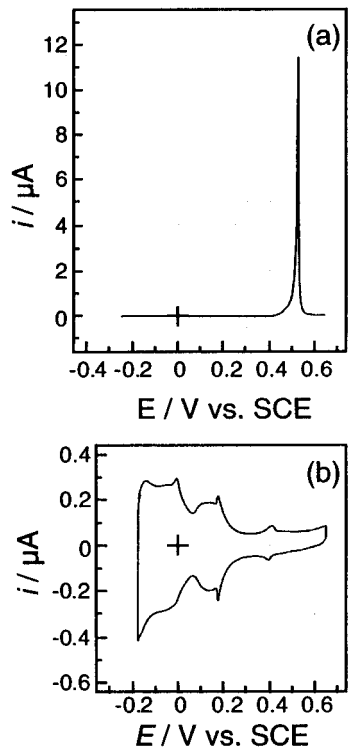

Figure 8. The long-time stability of the CO/Pt(111) electrode, which was kept for 60 min under dark. The electrochemical oxidation of CO (a) and the base CV after the CO oxidation (b).

Although much has been reported about the CO/Pt(111) system,[9−12,14,15] the atomic geometry corresponding to each peak in the voltammogram has not been established yet.[12] At the hydrogen UPD potential region, where the photodesorption was conducted in this experiment, Weaver and his group have found the two absorption bands in the infrared spectrum; the predominate sharp band at 2066 cm^{-1} and the weaker band centered at 1773 cm^{-1} were assigned to the atop coordinate CO and the CO adsorbed at the 3-fold-hollow sites, respectively.[14,15] Very recently, by X-ray diffraction technique using synchrotron radiation, Markovic and Ross have shown that the long range order appeared at the surface of CO/Pt(111) was p(2 × 2)-3CO, which is consisted of the atop CO and the CO trapped at the 3-fold-hollow site.[12]

In considering that (1) only the atop CO is able to be photodesorbed in the UHV case[5] and (2) the CO adlayer on Pt(111) electrode is consisted of atop CO and CO trapped at the 3-fold-hollow site,[12] the laser irradiation at 266 nm induces the photodesorption of the atop CO but the CO located at bridge or 3-fold-hollow sites do not desorb by the irradiation. The photodesorbed CO loses its kinetic energy very close to the surface and it is adsorbed again at the surface. Thus, this desorption and retrapping cycle decreases the population of the atop CO and increases the population of the CO adsorbed at bridge or 3-fold-hollow sites. This change in the molecular configuration at the CO layer induced the deformation of the CV shape for its electrochemical oxidation.

Acknowledgment. This work was partly supported by Research for the Future (RFTF) program by the Japan Society for the Promotion of Science. Authors thank Dr. E. D. Mishina for her critical reading of the manuscript.

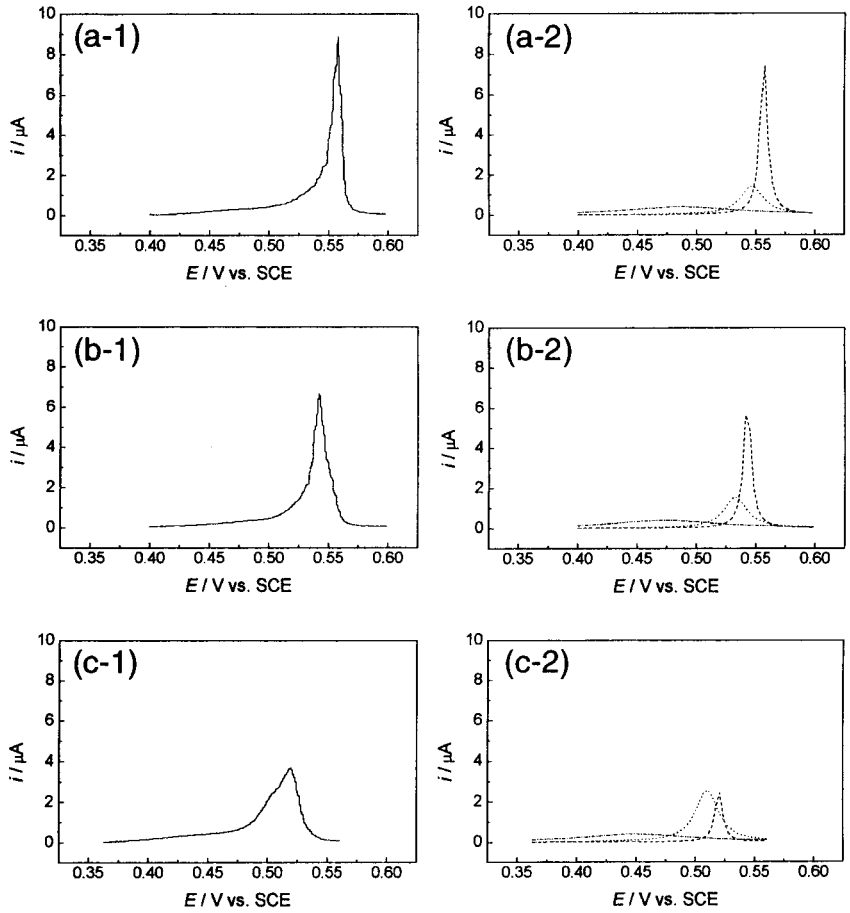

Figure 9. Deconvolution of theelectrochemical oxidation of surface adsorbed CO on Pt(111). The figures in the left column; (a-1) to (c-1), are the voltammograms identical with Figure 2a, b, and c, respectively. Those on the right, (a-2)−(c-2), are the deconvoluted results.

References and Notes

(1) Chuang, T. J. *Surf. Sci. Rep.* **1983**, *3*, 1.
(2) Betz, G.; Varga, P. *Desorption Induced by Electronic Transitions, DIET-IV*; Springer: Berlin, 1980.
(3) King, D. S.; Cavanagh, R. R. In *Advances in Chemical Physics*; Lawley, K. P., Ed.; Wiley: New York, 1989; Vol. 75, p 45.
(4) Zhou, X. L.; Zhu, X. Y.; White, J. M. *Surf. Sci. Rep.* **1991**, *13*, 73.
(5) Fukutani, K.; Song, M.-B.; Murata, Y. *J. Chem. Phys.* **1995**, *103*, 2221.
(6) Fukutani, K.; Murata, Y.; Schwarzwald, R.; Chuang, T. J. *Surf. Sci.* **1994**, *311*, 247.
(7) Buntin, S. A.; Richter, L. J.; King, D. S.; Cavanagh, R. R. *J. Chem. Phys.* **1989**, *91*, 6429.
(8) Dai, H. L.; Ho, W. *Laser Spectroscopy and Photochemistry on Metal Surfaces*; World Scientific: Singapore, 1995; Part II.
(9) Sun, S.; Clavilier, J.; Bewick, A. J. *J. Electroanal. Chem.* **1988**, *240*, 147.
(10) Gasteiger, H. A.; Markovic, N. M.; Ross, P. N. *J. Phys. Chem.* **1995**, *99*, 8290.
(11) Markovic, N. M.; Gasteiger, H. A.; Ross, P. N. *J. Phys. Chem.* **1995**, *99*, 3411.
(12) Markovic, N. M.; Grgur, B. N.; Lucas, C. A.; Ross, P. N. *J. Phys. Chem. B* **1999**, *103*, 487.
(13) Castell, R.; Reiff, S.; Drachsel, W.; Block, J. H. *Surf. Sci.* **1997**, *377*−*379*, 770.
(14) Villegas, I.; Weaver, M. J. *J. Chem. Phys.* **1994**, *101*, 1648.
(15) Leung, L. W. H.; Wieckowski, A.; Weaver, M. J. *J. Phys. Chem.* **1988**, *92*, 6985.
(16) Kolb, D. M. In *Spectroelectrochemistry*; Gale, R. J., Ed.; Plenum: New York, 1988; p 87.
(17) Misewich, J. A.; Heinz, T. F.; Newns, D. M. *Phys. Rev. Lett.* **1992**, *68*, 3737.
(18) Misewich, J. A.; Nakabayashi, S.; Weigand, P.; Wolf, M.; Heinz, T, F. *Surf. Sci.* **1996**, *363*, 204.
(19) Budde, F.; Heinz, T. F.; Loy, M. M. T.; Misewich, J. A.; de Rougemont, F.; Zacharias, H. *Phys. Rev. Lett.* **1991**, *66*, 3024.
(20) Peremans, A.; Tadjeddine, A.; Guyot-Sionnest, P. *Chem. Phys. Lett.* **1995**, *247*, 243.
(21) Peremans, A.; Tadjeddine, A.; Zheng, W.-Q.; Le Rille, A.; Guyot-Sionnest, P.; Thiry, P. A. *Surf. Sci.* **1996**, *368*, 384.